

Accelerating True-amplitude RTM of Deepwater Data Using Analytic Redatuming

Y. Qin and M. Okoniewski, Acceleware Ltd.

Introduction

The challenges for the exploration and production of hydrocarbons from the deepwater portion of the Outer Continental Shelf include high cost and a high level of environmental risk. Lowering the overall cost and risks of exploration in deepwater environments with complex salt formations depends critically on the accurate imaging of the salt geometry and sub-salt structure. Due to the large velocity contrast between the sediment and salt and the complexity of salt bodies, RTM has become the standard imaging tool to test different interpretation scenarios of the salt because of its high accuracy in modeling complex wave propagation. However, RTM is still an expensive tool. In the case of applying RTM to deepwater offshore areas, a significant portion of the total runtime is used to propagate wavefields through the low-velocity water layer. Since the velocity in the water is typically homogenous or has very small vertical variation, in this paper, we employ analytical redatuming to accelerate deepwater RTM. The idea is to analytically-redatum the source and receiver wavefields to the depth of the water bottom, and then migrate the redatumed source/receiver wavefields using RTM to image the region below the water bottom.

Theory

The first step in employing analytical redatuming to accelerate RTM in deep water, is to divide the velocity model into two layered regions close to, but above, the water bottom. We refer to the plane along which the two regions are divided as the “redatum depth”. For the top water layer with near-constant water velocity or very small vertical velocity gradient, the source and receiver wavefields are analytically propagated to the redatum depth. Thus, a point source on the surface becomes an areal source at the subsurface datum. The analytically-redatumed source/receiver wavefields at the redatum depth become the input for the shot-domain RTM to image the region below the water bottom.

In a 3D model, the source wavelet is analytically redatumed to the redatum depth as

$$S(\mathbf{x}_d, t) = \frac{1}{4\pi v^2} \mathbf{w}(t - |\mathbf{x}_d - \mathbf{x}_s|/v + d/v)/|\mathbf{x}_d - \mathbf{x}_s| \quad (1)$$

where $S(\mathbf{x}_d, t)$ is the redatumed source wavefield at the point \mathbf{x}_d on the redatum depth d ; \mathbf{x}_s is the 3D location of the actual source; \mathbf{w} is the source wavelet time signature; v is the water velocity.

The receiver traces are analytically backward redatumed to the redatum depth as

$$R(\mathbf{x}_d, t) = \frac{1}{4\pi v^2} \int \frac{D'(t + |\mathbf{x}_d - \mathbf{x}_r|/v + d/v) \cos(\alpha_0^r)}{|\mathbf{x}_d - \mathbf{x}_r| v} d^2 \mathbf{x}_r \quad (2)$$

where $R(\mathbf{x}_d, t)$ is the backward redatumed receiver wavefield at the point \mathbf{x}_d on the redatum depth d ; \mathbf{x}_r is the 3D coordinate of actual receivers; D' is the fully-differentiated receiver data, where full differentiation is applied to guarantee that the phase and amplitude of the redatumed data are correct; v is the water velocity; α_0^r is the emergent angle at each receiver location. It needs to be pointed out that the directional correction factor $\frac{\cos(\alpha_0^r)}{v}$ should be incorporated while backward redatuming receiver wavefield for common-shot RTM (Qin & McGarry, 2013).

The redatumed source is forward propagated as

$$P_D(\mathbf{x}; \omega) = \int S(\mathbf{x}_d; \omega) G(\mathbf{x}_d, \mathbf{x}; \omega) \frac{i\omega \cos(\alpha_d^s)}{v_d^s} d^2 \mathbf{x}_d \quad (3)$$

where $P_D(\mathbf{x}; \omega)$ is the propagated source wavefield below the redatum depth; $G(\mathbf{x}_d, \mathbf{x}; \omega)$ is the Green function between redatumed source wavefield \mathbf{x}_d and image point \mathbf{x} ; v_d^s and α_d^s are the velocity and the incidence angle at each redatumed source. Again, it needs to be pointed out that the directional term $\frac{\cos(\alpha_d^s)}{v_d^s}$ should be incorporated into the forward propagation of redatumed source wavefield.

The redatumed receiver is backward propagated as

$$P_U(\mathbf{x}; \omega) = \int R(\mathbf{x}_d; \omega) G^*(\mathbf{x}_d, \mathbf{x}; \omega) \frac{i\omega \cos(\alpha_d^r)}{v_d^r} d^2 \mathbf{x}_d \quad (4)$$

where $P_U(\mathbf{x}; \omega)$ is the propagated receiver wavefield below the redatum depth; $G^*(\mathbf{x}_d, \mathbf{x}; \omega)$ is the complex conjugate of the Green function between redatumed receiver \mathbf{x}_d and image point \mathbf{x} .

To illustrate the necessity of the directional terms in equations (3) and (4), we compare the snapshots of source wavefield after injecting the redatumed source wavefield in a constant velocity with and without this directional correction. As seen in Fig. 1a and 1c, the amplitude of source wavefield is spherically symmetric as expected when the directional term is applied. Without this directional term, Fig. 1b and 1d show that the amplitude of source wavefield increases with increasing incidence angle.

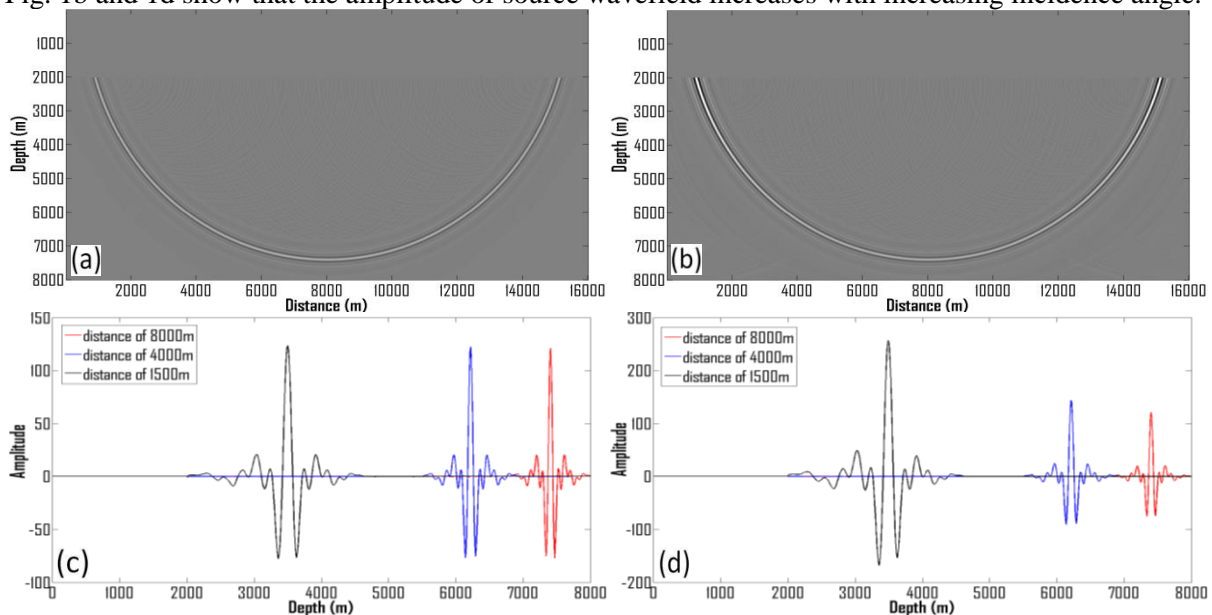


Figure 1: Snapshot of source wavefield after injecting the redatumed source wavefield with directional correction (a) and without directional correction (b). (c) and (d) compare some of traces in (a) and (b), respectively.

Numerical and field examples

To show that our analytical-redatuming RTM produces true-amplitude images, we first applied regular true-amplitude common-shot RTM (Qin & McGarry, 2013) and analytical-redatuming RTM to a 2D synthetic model with 3 density-contrast reflectors and constant velocity of 3000m/s. These 3 reflectors have the same theoretical angle-independent reflectivity. The input synthetic shot gather is generated by assuming the amplitudes of recorded reflection events are only affected by geometrical spreading as shown in Fig. 2a.

The analytically-redatumed receiver and source wavefields are shown in Fig. 2b and 2c. Clearly, the length of the redatumed receiver wavefield is much shorter, and thus the runtime is significantly reduced. It can be noted that a point source becomes an line source (area source for 3D case) after redatuming for shot-based RTM. The redatumed source and receiver wavefields at a depth of 1900m were used to generate the image shown in Fig. 3b.

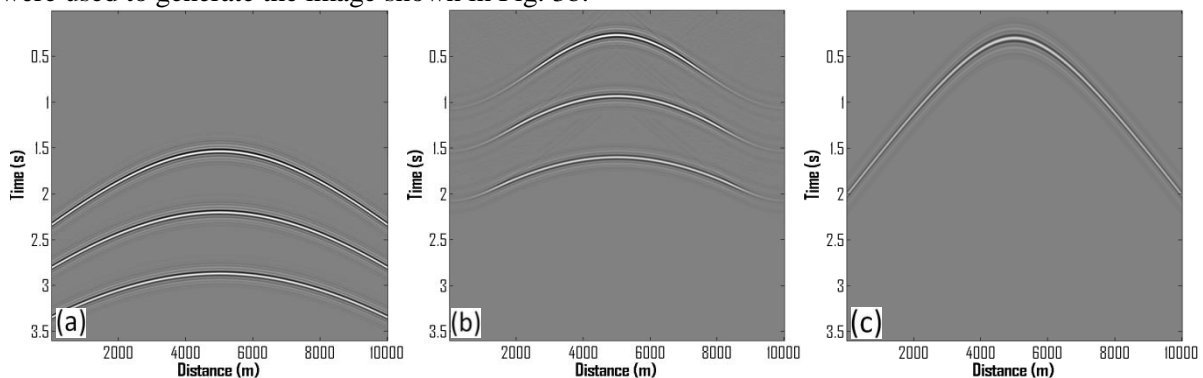


Figure 2: (a) original receiver traces at the surface. (b) receiver wavefield after redatuming to depth of 1900m. (c) source wavefield after redatuming to depth of 1900m

Figures 3a and 3b show the shot image of regular true-amplitude RTM and analytically-redatumed true-amplitude RTM, respectively. Figures 3c and 3d show the corresponding picked peak amplitudes along the 3 imaged reflectors, which match well with the theoretical reflectivity.

Since the depth of the water bottom can vary significantly, particularly for surveys close to the shore, the redatuming depth needs to vary shot-by-shot in order to improve RTM efficiency as much as possible. Therefore, it is important to make sure that the amplitude of each shot image is not affected by the redatum depth. Figure 4 shows the effect of redatum depth on the amplitude of the imaged reflector at the depth of 3km. It can be seen that the amplitude of the RTM shot image using different redatum depths is nearly the same.

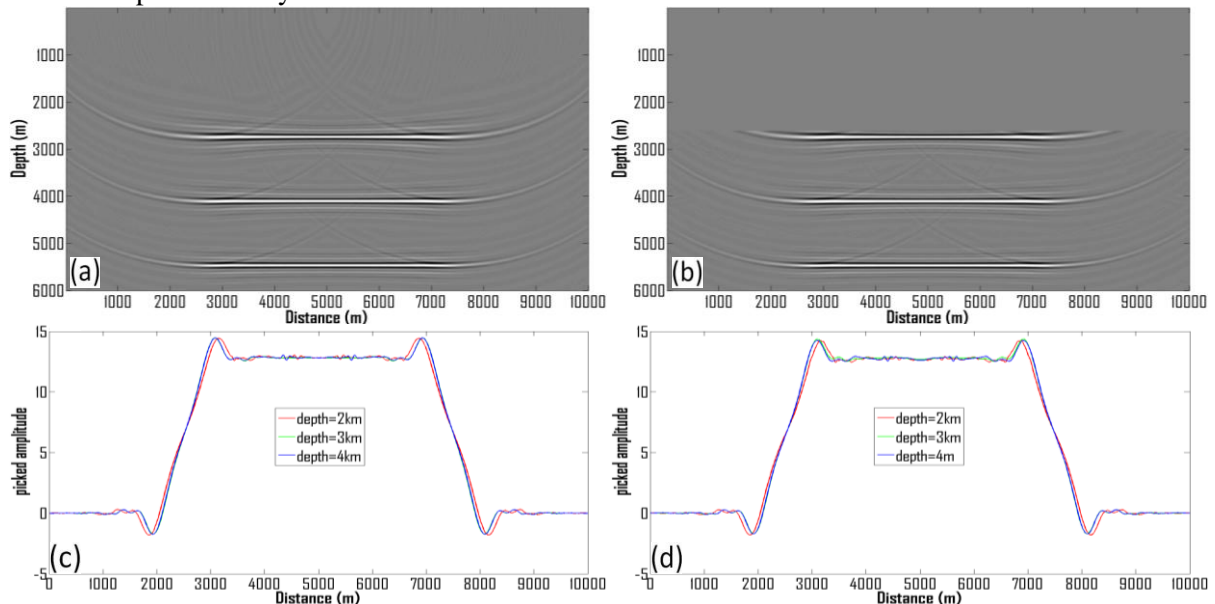


Figure 3: (a) Shot image of regular true-amplitude RTM. (b) Shot image of true-amplitude RTM using analytical redatuming where redatum depth is 1900m. (c) Peak amplitude along the 3 imaged reflectors in (a). (d) Peak amplitude along the 3 imaged reflectors of shot image shown in (b). The model has 3 horizontal density-contrast reflectors and constant background velocity of $v=3000\text{m/s}$.

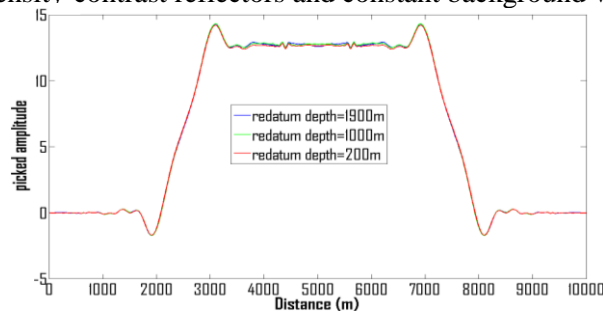


Figure 4: Peak amplitude of the reflector at depth of 3km, imaged by analytical-redatuming true-amplitude RTM for different redatum depths at 1900m, 1000m and 200m, respectively.

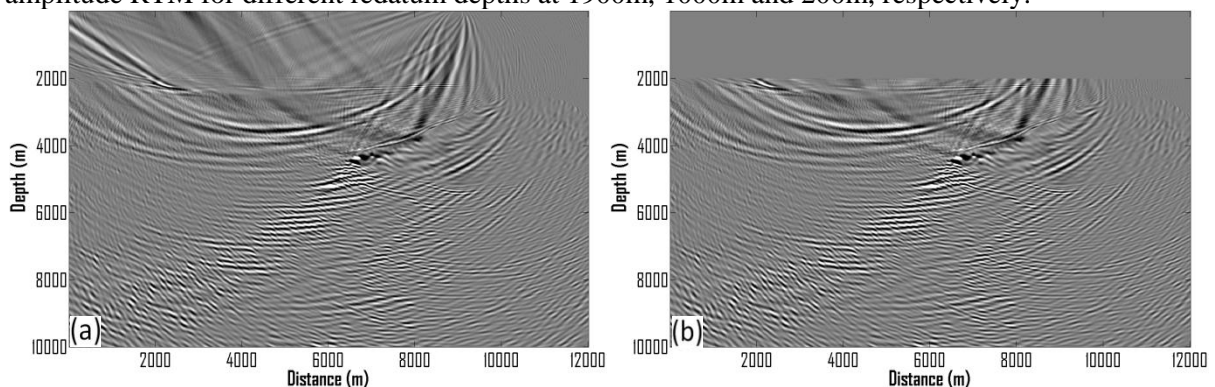


Figure 5: Comparison of regular true-amplitude RTM (a) and analytical-redatuming true-amplitude RTM (b), using the same field velocity model with salt body close to water bottom.

The second example is a complex 2D field model with a salt body, in a deep-water region of Gulf of Mexico. Figure 5 shows the raw shot image using regular true-amplitude RTM and the analytical-redatuming true-amplitude RTM. These 2 images are almost identical, including the turning-wave self-correlation noise and the top-of-salt reflection low frequency noise. The comparison of the image traces at a distance of 7700m is shown in Fig. 6a, where the small difference can be attributed to the singularity of point source injection in finite difference method. As a contrast, Fig. 6b shows the similar comparison, but the redatumed source and receiver wavefields are generated by finite-difference propagation. After removing the effect of singularity with point source injection in FDM, the waveform of the image traces at distance of 7700m look almost identical. Fig. 6b also shows that the proposed propagation of redatumed wavefield based on equations (3) and (4) can be directly used for developing true-amplitude layer-stripping RTM.

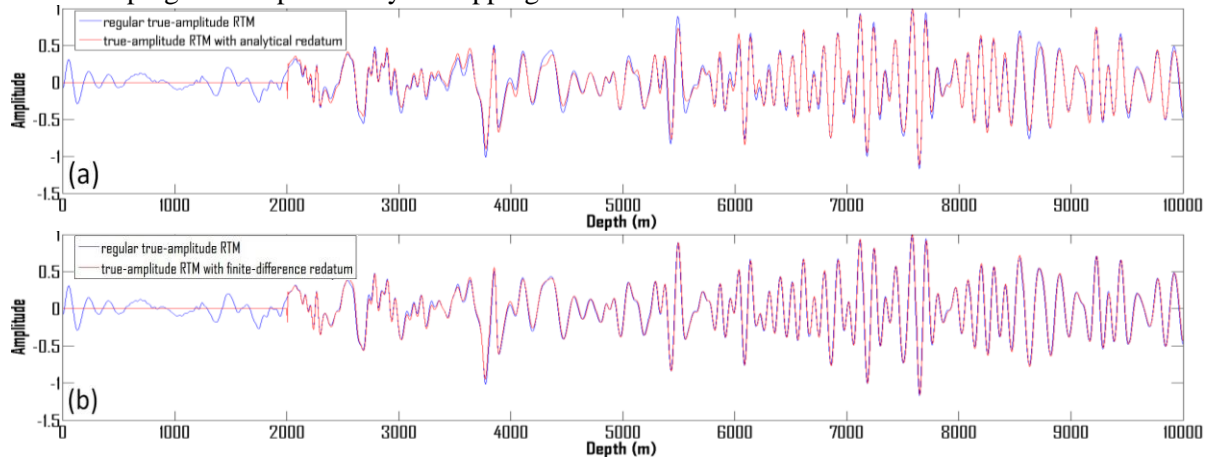


Figure 6: Comparison of the image trace at distance=7700m. (a) regular true-amplitude RTM and true-amplitude RTM with analytical redatuming. (b) regular true-amplitude RTM and true-amplitude RTM with finite-difference redatuming.

Discussion

With analytical redatuming, point source injection is replaced by injecting the analytical surface source solution into the finite-difference (FD) grid, and so the singularity of point source injection in the conventional FD computation is avoided. Regular FDM forces the location of source and receiver to the center of nearest cell. Through analytical redatuming, accurate positioning of source and receivers is naturally incorporated without any extra cost. Grid dispersion effects related to the deep water layer are also eliminated. Because the computational cost of analytical redatuming is negligible compared to numerical wave propagation in RTM, the analytical redatuming can be done on the fly, which eliminates any potential I/O bottleneck. In case that the water velocity has slight vertical variation, the harmonic average velocity or effective vertical transverse isotropic velocity is used to calculate the traveltimes during the analytical redatuming.

Since the relative amplitudes are maintained during the redatuming of the source and receiver wavefields and propagating redatumed wavefield, the approaches described in this paper can also be extended to accelerate full-waveform inversion (FWI) and true-amplitude common-angle RTM, and used for developing true-amplitude layer-stripping RTM.

Conclusions

In this paper, we have presented a method to analytically redatum both the source and receiver wavefields and inject the redatumed wavefield into the computational domain while maintaining true-amplitudes in the migrated common-shot image. The main benefits of analytical-redatuming, true-amplitude RTM, are to reduce runtime, memory and disk space requirements for deepwater imaging and thus enable higher-frequency RTM to be run using existing computer hardware. Among other benefits are the ability to overcome the singularity of point-source injection in the finite difference method, accurate positioning of source and receivers, and the reduction of numerical dispersion noise.

References

Qin, Y., and R. McGarry, 2013. True-amplitude common-shot acoustic reverse time migration. 83rd annual SEG meeting, Expanded Abstracts, 3894-3899